Multibody simulation of derailment risk in railway switches due to gauge narrowing caused by foreign objects

Citation for the original published paper (version of record):
Bysani, S., Pålsson, B., Kabo, E. (2025). Multibody simulation of derailment risk in railway switches due to gauge narrowing caused by
foreign objects. Vehicle System Dynamics, In Press.
http://dx.doi.org/10.1080/00423114.2025.2495227

(article starts on next page)

Vehicle System Dynamics
International Journal of Vehicle Mechanics and Mobility

ISSN: 0042-3114 (Print) 1744-5159 (Online) Journal homepage: www.tandfonline.com/journals/nvsd20

Multibody simulation of derailment risk in railway switches due to gauge narrowing caused by foreign objects

Sucheth K. K. Bysani, Björn A. Pålsson & Elena Kabo

To cite this article: Sucheth K. K. Bysani, Björn A. Pålsson & Elena Kabo (05 May 2025): Multibody simulation of derailment risk in railway switches due to gauge narrowing caused by foreign objects, Vehicle System Dynamics, DOI: 10.1080/00423114.2025.2495227

To link to this article: https://doi.org/10.1080/00423114.2025.2495227

Published online: 05 May 2025.

VEHICLE SYSTEM DYNAMICS
https://doi.org/10.1080/00423114.2025.2495227

OPEN ACCESS Check for updates

Multibody simulation of derailment risk in railway switches due to gauge narrowing caused by foreign objects

Sucheth K. K. Bysani, Björn A. Pålsson and Elena Kabo

Department of Mechanics and Maritime Sciences/CHARMEC, Chalmers University of Technology, Gothenburg, Sweden

ABSTRACT

Railway switches are essential for ensuring efficient train operations, and efforts to improve their safety standards have driven the introduction of 'switch rail control contact' (TKK in Swedish) sensors in Sweden. These sensors monitor the gap between the switch and stock rail, complementing the switch rail position detection of the drives. Despite their benefits, TKK sensors are prone to faults, which in turn increase maintenance and operational costs. This study was therefore initiated to assess the utility of these devices in derailment prevention. To assess the risk of derailment caused by gauge narrowing induced by entrapped foreign objects, multibody simulation (MBS) of train switch interactions is performed. A state-of-the-art structural track model of a switch is modelled in Simpack. Simulations indicate that the train will not derail due to flange climbing when the foreign object is modelled with a failure criterion resembling crushing strength of ballast stones. An investigation featuring an unbreakable object showed that the critical gauge narrowing limit considering flange climbing is around 15 mm which is in accordance with the existing safety limit. The influence of track irregularities in combination with foreign objects is also investigated.

ARTICLE HISTORY
Received 28 October 2024
Revised 6 March 2025
Accepted 10 April 2025

KEYWORDS
Railway switch; multibody simulations; derailment risk; structural track modelling; foreign object

Introduction

Switches are essential for railway operations as they allow for trains to change track. They are also critical because they include moving switch rails that must be moved to and then be locked in the correct position to guide trains into the intended route [1,2]. The actuation required to achieve this make switches more prone to faults compared to tangent track [3]. The outline of a common Swedish switch and crossing (S&C) of radius 760 m is shown in Figure 1. Green rails indicate the through route, while blue rails indicate the diverging route. The switch rails are connected to each other by means of three long cylindrical bars called links. They are indicated by dashed lines in Figure 1. Their function is to increase the bending stiffness of the switch rails by connecting them in parallel and to ensure that the distance between the switch rails remains fixed. The switch rails are supported vertically by sleeper mounted slide chairs and rollers to enable smooth operation. Actuation of the switch rails are carried out by the two drives indicated in orange. They exert a force of

CONTACT Sucheth K. K. Bysani sucheth.bysani@chalmers.se

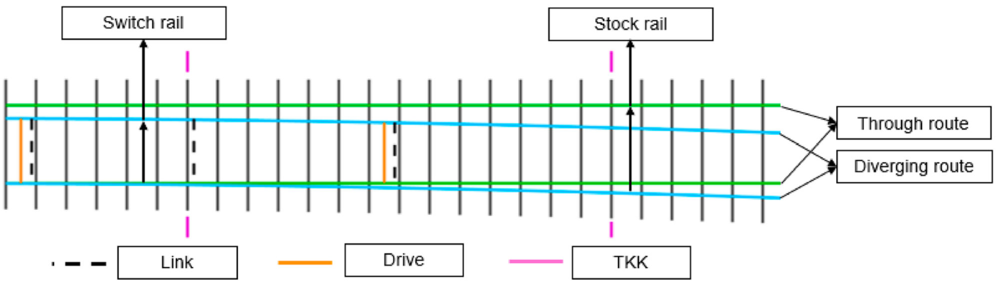

Figure 1. Overview of a UIC60-760-1:15 S&C in Sweden.

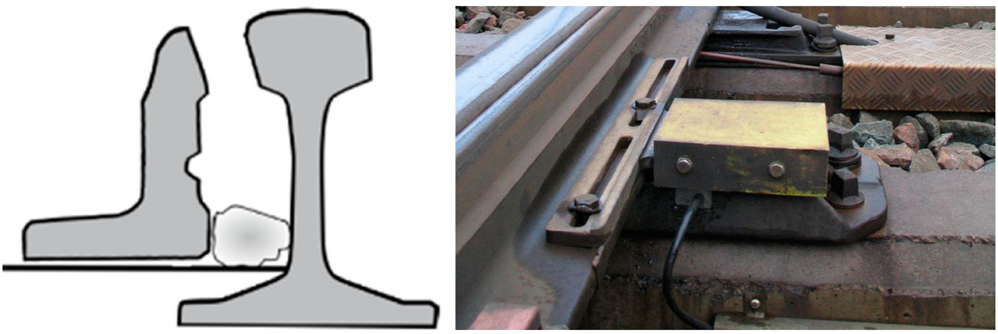

Figure 2. Cross-section of switch and stock rail with interfering foreign object [11]. Right: Picture of TKK sensor used in field [12].

maximum 6 kN each to actuate the switch [4,5]. Drives are in control if the gap between the switch and stock rail at the drive should be less than the upper tolerance limit of 5 mm [6]. Gaps between switch and stock rails are monitored at four locations using so-called TKK sensors (indicated by purple colour). TKK is a Swedish abbreviation for 'switch rail control contact' [6–8]. The control limit of the TKK is 13 mm [6]. A picture of a TKK in track can be seen in Figure 2. The number of TKKs needed varies depending on switch radius and drive configurations.

One type of fault is when foreign objects find their way in between switch rail and stock rail as shown in Figure 2 [1]. These objects are for example ballast stones or ice from passing trains. When the switch alters position, the object will prevent the switch rails from fully closing, thus resulting in gauge narrowing that can lead to derailment due to flange climbing if not detected [7,9]. To prevent this from happening, the switch rail will only be in control in the signalling system and traffic be allowed, if the switch rail is locked at the drives and the TKK sensors are within the tolerance limit. This means that the gap between switch and stock rail is not greater than 5 mm at the drives and 13 mm at the location of the TKK sensor. The system is designed to detect objects that cause a gauge widening exceeding 15 mm as standards specify that to be safe [10]. If the TKK sensors are removed, gauge widening between 25 and 30 mm can be present, while the drives are still in control [11].

The challenge with locking detection at drives and TKKs is their reliability. They can sometimes indicate faults even when there are none, which can result in traffic disruptions. To get an overview of the situation, data from Trafikverket's (The Swedish Transport

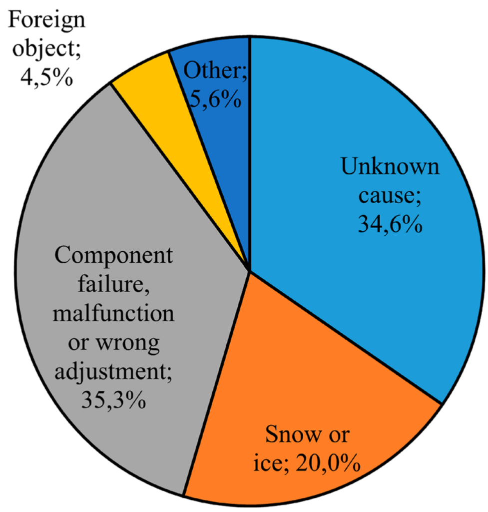

Figure 3. Categorisation of faults associated with control of switches in Sweden based on data from Trafikverket for the year 2017.

Administration) database of railway infrastructure faults (Ofelia) was analysed for the full year of 2017. In total there were 8597 faults related to S&Cs in Sweden. By searching for keywords such as 'switch not in control' and 'switch not going into position', etc. in the error description, 4853 faults were found. Given that the identification stems from free-text searches the identification accuracy is not perfect, but by inspecting samples of the identified and remaining issues, it was concluded that most of the not-in-control cases had been identified. It can thus be noted that a bit more than half of S&C faults were related to not-in-control switches.

Studying the associated reported causes for not-in-control switches, no root cause was found in 35% of the cases, and the action taken here is typically lubrication, adjustment or additional inspections. In 35% of the cases faults were related to component failure, malfunction or wrong setting and following repair or adjustment. Out of these 1711 faults, 201 are associated with TKKs. In 20% of the cases, the problem was snow or ice and in 5% of the cases it was a foreign object. 5% are faults that are not easily associated with the other categories, such as damage from maintenance equipment, thunderstorms and so on.

Studying the snow and ice and foreign object categories together, it was found that in 94% of the cases with these causes, the action taken was clearance, snow clearance or cleaning, confirming that there was indeed stuck material preventing the switch from going in control. For the foreign object category, the type of object is sometimes mentioned, and ballast stones are by far the most common type. There are also instances of wood, animals, tarps, etc., as well as metal objects such as detached switch heating elements. A breakdown of the fault categories can be seen in Figure 3.

As the system does not register if a not-in-control case was caused by the drives or the TKKs, it is not possible to determine how many of the 1188 cases of snow, ice and foreign objects that were triggered by a TKK. It is, however, reasonable to assume that the TKK contributes to a significant part as it is required to detect interfering objects along large parts of the switch rails as shown in [11]. Together with the faults in the TKK sensors themselves, it is estimated that TKKs contribute to 500–1000 not-in-control cases in Sweden per year. If it can be demonstrated that these types of interruptions do not pose a derailment risk, TKKs could potentially be omitted from the switch control system. This would not only reduce the overall number of control errors in switches but also lower maintenance and operational costs.

To address these scenarios, multibody simulations (MBS) are performed to determine the response of the switch rail system and the train in cases of trapped foreign objects. The aim is to assess the potential for derailment in these cases. To this end, this paper will address three research questions based on the presumption that the TKK sensor is removed and gauge narrowing up to 25 mm can be present during traffic [11].

(1) What is the risk of derailment when the gauge narrowing is caused by a trapped ballast stone or by an infinitely strong object placed at the foot of the switch rail?
(2) What is the robustness of the findings for derailment risk with respect to axle load, wheel–rail friction coefficient and vehicle speed?
(3) What is the maximum gauge narrowing that can be tolerated without a risk of derailment due to flange climbing?

With the answers to these questions, we hope to contribute to better understanding of derailment risks in switches due to trapped foreign objects and also provide a more solid foundation for the design of a robust system for switch rail control.

Modelling requirements

To address the posed research questions using simulations, an appropriate simulation model needs to be created. As the evaluation of dynamic vehicle–switch interaction is required, MBS is a natural choice. A structural (finite element (FE)) track model is required in MBS for realistic results as the switch rail has many different discrete support points and connections along its length (slide chairs, stock rail contacts, drives and links) that need to be accounted for together with the bending stiffness of the rail. The switch rail cross-section dimensions and the locations of acting forces need to be accounted for as the acting forces can cause torsion about the switch rail's longitudinal axis. This will change the gauge and wheel–rail contact conditions. It is also necessary to simulate the actual switching operations to create correct initial conditions with trapped objects before vehicle passage.

State-of-the-art

This section will explore previous works and the state-of-the-art of simulations in relevant areas. These are structural track modelling of S&C, switching operations and derailment risk analyses.

Structural track modelling of S&C

Numerical simulations of vehicle–S&C interaction remain a highly active area of research, with a wide range of modelling techniques available to accurately predict this complex interaction. Several studies, such as those in [13,14], employ the co-simulation method where a separate FE track model is coupled to an MBS vehicle model in simulation. Others, including [15,16], utilise the co-running track model where a mass-spring-damper system under each wheelset is used to represent the dynamic track properties. There is also the possibility of using an FE-type track model representation in the MBS model, for example by using the modal superposition method [17–19] or by using beam elements or reduced order models to represent rails and sleepers [20–23]. The only study found that accounts for the non-linear contacts and sliding friction between switch rail and stock rail and baseplate was [24] in a co-running track model. For further comparison of modelling techniques in S&C, see for example Pillai et al. [25] or Pålsson et al. [26].

Switching operations

Duta et al. in [27,28] developed a self-adjusting railway switch system model which works on a closed loop control system that re-adjusts itself to close any gap. In their switch system model, the switch rail is modelled as a flexible body in an MBS software Simpack [29] by using bodies created in an FE software, i.e. ABAQUS [30]. The closed loop system consists of a co-simulation between Simulink and Simpack models. An extension to the previous study [28] was done by Li et al. [31]. They combined an actuator model developed in Simulink and a validated FE model of a switch rail [30], to validate it against steady-state predictions from an MBS model of a railway switch developed in Simpack. In [32], the authors extended their previous work to develop a framework for dynamic modelling of switches by taking into consideration the switch blades, actuators and control systems. The novel actuation system ensures a continued operation even with a single actuator failure. The influence of foreign objects on switch rail operations has been investigated by developing a novel FE model in ABAQUS that simulates switching operations in the presence of interfering objects [11].

Derailment risk in S&C

Derailment of a train passing through an S&C have for long been a concern, resulting in research of ways to predict and take necessary actions to prevent it. Wang et al. in [33] developed a derailment coefficient criterion for S&Cs considering the influence of creep force and wheelset yaw angle. Lai et al. in [34] developed an MBS model in Simpack to investigate derailment risk when empty wagons pass through a switch under a braking force applied by a vehicle retarder. The influence of longitudinal force of other wagons, wheel–rail friction coefficient and vehicle speed on the derailment risk are also investigated in this study. Jiang et al. in [35] make use of an MBS model developed in Simpack to investigate the mechanism of flange climbing derailment of an empty wagon passing through a S&C in the diverging route. The authors conclude that the longitudinal coupler force and the wheel–rail friction coefficient are major influencing factors. They also suggest the implementation of a guard rail before the switch to reduce derailment risk by flange climbing. In continuation to the previous studies, Lai et al. in [36] utilised a Simpack model to investigate the influence of rail joints placed before a S&C on the derailment risk and analysed the effects of different parameters such as S&C radius, wheel–rail friction coefficient and gap between the rail joint and switch rail toe on the derailment risk.

Outcomes of the literature review

From the literature review, it is concluded that no previous publications have investigated risks of derailment due to foreign object interference in railway switches. In terms of modelling, it can be concluded that there have been simulations with actuated flexible switch rails that account for the switch rails different discrete contacts and connections (slide chair and stock rail contact, links and drives), but only for the analysis of switching operations, not for dynamic vehicle–switch interaction. Also the switch rail torsion has not been investigated in this context. Both the research topic and the modelling approach are therefore novel.

Multibody model

The MBS model for the study of dynamic vehicle–switch interaction is built in the commercial software Simpack [29]. The model includes a structural representation of the switch panel of a UIC60-760-1:15 S&C and preceding tangent track, modelled in the non-linear flextrack module of Simpack. Traffic is represented by the Manchester benchmark passenger vehicle model [37] with an axle load of 11 t. An overview of the Simpack model can be seen in Figure 4 and a schematic top view of the model is presented in Figure 5.

The tangent track is modelled using only rails while the switch panel includes the full track structure with rails and sleepers. Both the rails and sleepers are modelled as flexible bodies. This simplification is made to reduce computational efforts as there are no dynamic

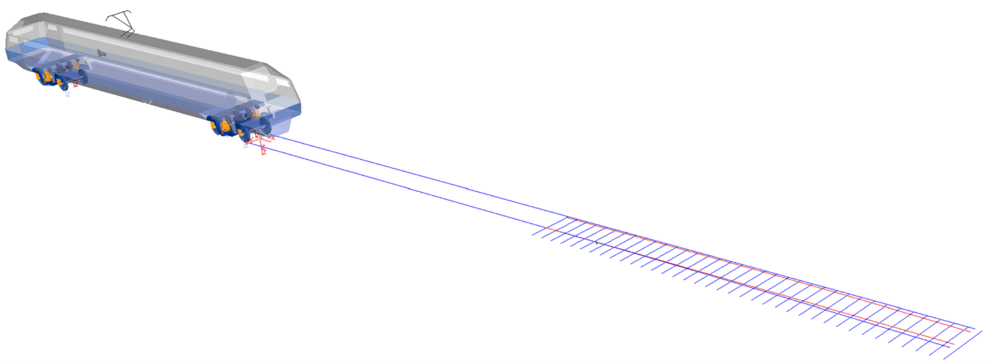

Figure 4. MBS model of vehicle–switch interaction in Simpack.

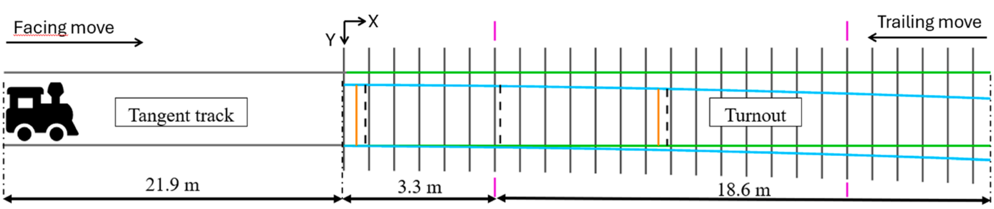

Figure 5. Illustration of the MBS model setup, featuring a tangent track leading into the S&C. Refer to Figure 1, for details about the S&C. Origin of the track model coordinate system is at the start of the S&C.

excitation on the tangent track making it unnecessary to include the sleeper bodies. The support stiffness of the tangent track is adjusted to give the same track stiffness as that of the start of the switch panel to ensure a smooth transition. Rails and sleepers are constructed using Timoshenko beam elements. The varying properties of the switch rails due to their tapered ends are accounted for. This implies reduced mass and bending stiffness towards the rail ends [26]. All rails and sleepers are condensed into super elements using a Craig–Bampton reduction [38].

The connections between rails and sleepers are modelled using linear bushing (Kelvin) and force elements. Each sleeper is supported by a discretised system of independent bushings in the vertical direction. This represents the distribution of stiffness and viscous damping of the ballast and subgrade (Winkler bed). The stock rails in the switch panel are connected to the sleepers with bushing elements and the rails in the tangent track are connected with bushings to ground.

For the switch rails on the other hand, the situation is more complex as these are constrained by a combination of rail fastenings, contact surfaces and locking devices. The different constraint regions are illustrated in Figure 6. All contact surfaces account for normal and tangential contact forces.

Both the through and diverging switch rails are connected to the sleepers in the same way as the stock rails in the 'switch rail fastening region' at the right end of the switch panel in Figure 6. For the rest of its length, the switch rails are supported by contacts to the sleeper mounted slide chairs in the vertical direction. The sliding contacts in this region are established by using the 'universal point contact' element with a friction coefficient of 0.1 [11]. In the lateral direction, there are two different contact regions. One is the 'switch to stock rail contact region' where the switch rail has an inclined contact surface to the stock rail close to the top of rail (ToR). The intermediate 'stock rail knob contact region' has contact elements defined between stock rail and switch rail purely in the lateral direction mimicking the stock rail knob supports for the switch rail. Nominal input parameters to the MBS model are presented in Table 1.

Links as seen in Figure 1 are long cylindrical bars connecting the through and diverging switch rails with pivoting bolt connections. There are three links in the present switch design. The links are modelled as linear springs of 1.5 kN/mm stiffness. The value of the link stiffness was obtained via FE simulations of the link geometry in ABAQUS.

Drives and foreign object are modelled using force elements. The two drives are modelled exerting a lateral force of 6 kN against the switch rail as seen in Figure 6. In time domain simulations with passing vehicles, the switch rail is locked at the drive positions with bushing elements with a stiffness of 10 kN/mm in the lateral direction. The foreign object modelling is presented in the following section. The foreign object is positioned at the location of the front TKK in the facing move, which is approximately equidistant from both drives. This placement represents the most critical region where the largest foreign object could potentially go undetected by the drives alone, without the presence of the TKK. As the foreign object is moved towards the drives the probability of it getting detected increases significantly [11].

Even though the switch rail itself is modelled using beam elements, the spatial dimensions of its cross-sections are accounted for to give realistic contact conditions, especially under torsional deformation. The switch rail contact cross-sections are defined by four nodes, one at the top of rail, two at the bottom of rail and one at the centre of the mass/beam

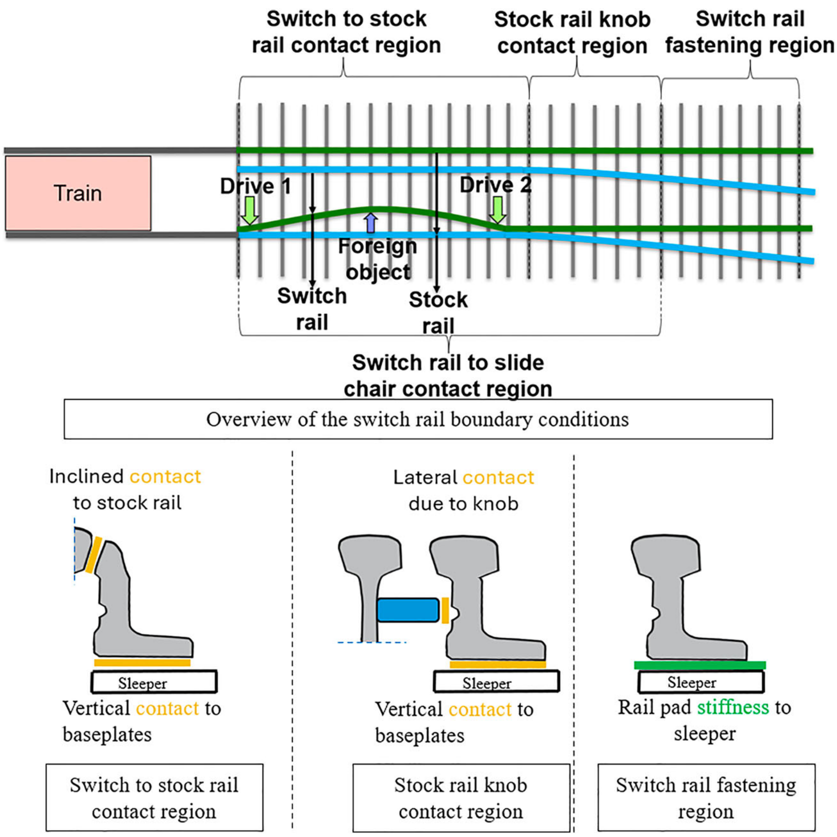

Figure 6. Overview of the applied forces, foreign object interference, contacts and fastening regions applied on the switch rail. Bottom: Cross-sectional view of the contact and fastening conditions for different sections of the switch rail.

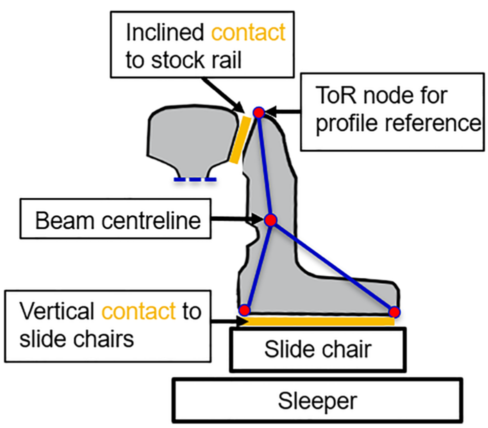

Figure 7. Switch rail cross-section with four nodes. Vertical contact to sleepers and inclined lateral contact to stock rail.

Table 1. Nominal MBS parameters and values.

MBS model components		Type/value
Vehicle	Type	Carbody with two bogies [37]
	Wheel profile	S1002
	Wheel radius [m]	0.46
	Wheelset mass [kg]	1813
	Axle load [kg]	11,000
Rail	Element type	Timoshenko beam
	Node spacing along rails in MBS [m]	0.6
	Profile	UIC60/60E1
	Young's modulus [GPa]	210
	Nominal mass density [kg/meter rail]. The tapered switch rails have the space dependent properties defined in [26]	60
	Track gauge	1435 mm
Sleeper	Structural element type	Timoshenko beam
	Node spacing along body [m]	0.6
	Young's modulus [GPa]	45
	Mass density [kg/m^3]	2400
Ballast bed	Bushing element type	Kelvin bushing elements
	Vertical and lateral stiffness per meter of sleeper [MN/m/m]	30
	Vertical damping per meter of sleeper [kNs/m]	50
Stock rail and switch rail fastenings	Type	Kelvin bushing elements
	Translational and rotational stiffnesses in all directions [MN/m]	50 [22]
	Translational and rotational damping in all directions [KNs/m]	10
Switch rail to base plate contact region	Element type	Universal point contact
	Normal axis	Vertical
	Friction coefficient	0.1
Switch to stock rail contact region	Element type	Universal point contact
	Normal axis	Lateral
	Friction coefficient	0.3
Stock rail knob contact region	Element type	Unilateral spring
	Normal axis	Lateral

centre line as presented in Figure 7. The nodes are connected by rigid links. Contacts are defined between the top node of the cross-section and the inclined surface of the stock rails as well as vertical contacts between bottom nodes and the sleeper mounted slide chairs.

Foreign object modelling

Ballast stones and ice are the most common types of foreign objects that get stuck between the switch and stock rail [9]. Occasionally, metal objects from the train or other sources such as switch heating elements also get stuck, thus acting as foreign objects. Given that ballast stones and metal objects are the strongest and most severe discrete objects, this study will replicate their behaviour. Ice and ballast stones exhibit a similar behaviour, as they both get crushed once a certain force is applied [39]. The Young's modulus and compressive strength of ice are 9.7–11.2 GPa and 5–25 MPa, respectively. Compressive strength of ice is dependent on temperature, strain rate, tested volume and ice grain size [40]. Ballast stone

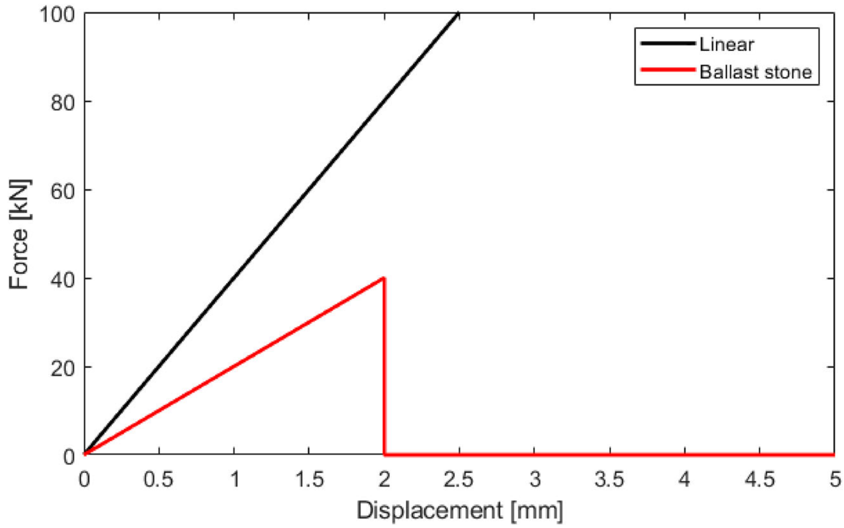

Figure 8. A force–displacement relation for linear and ballast object formulations.

has a Young's modulus of 50 GPa and compressive strength of around 60 MPa (depending on the shape of the ballast stone) [41]. Therefore, a ballast stone scenario should be more conservative with a greater derailment risk compared to pieces of ice as ballast stones are stronger. Continuous build-up of snow and ice along the switch is normally prevented by switch heating.

Tests on the crushing of ballast stones and comparison to finite element (FE) simulations were performed in [41] and [42]. Based on the force versus displacement curves in [41] and [42], it was observed that the maximum force a ballast stone could withstand ranged from approximately 35 to 45 kN. To replicate this behaviour, a failure criterion was incorporated into the foreign object description within Simpack. Two different formulations with varying energy absorptions were modelled:

(1) Linear variation: An infinitely strong object is represented as a spring with a lateral stiffness of 40 kN/mm. This setup represents a practically unbreakable object (e.g. a metal object) that will not fail under the applied forces.
(2) Ballast stone variation: Failure criterion is introduced for the object when the applied force reaches 40 kN. This scenario represents a ballast stone of average strength that will disintegrate once it reaches the crushing force. A stiffness of 20 kN/mm is defined for the proportional region [42].

The force–displacement behaviour of these object models is illustrated in Figure 8. By incorporating these different variations, the simulation aims to capture the behaviour of foreign objects with varying energy absorptions and provide insights into the resulting transient events as the train passes through the switch. An object that gives a gauge narrowing of 30 mm is studied corresponding to the gauge narrowing induced during measurements and represents the worst-case scenario without the TKK [11].

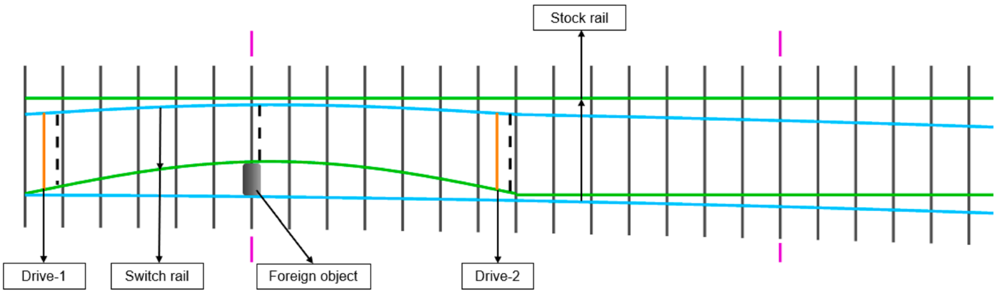

Figure 9. Switch rail deformation caused by the introduction of a foreign object and application of drive forces.

Simulation procedure

To simulate the effects of a foreign object, the following simulation procedure is applied:

(1) The model is brought to static equilibrium with the switch positioned in the through route and the vehicle on tangent track.
(2) The foreign object is introduced as a prescribed displacement that separates the switch and stock rail at the object location with the prescribed object size. The foreign object is introduced at the foot of the switch rail and at the front TKK location. Drives are inactive in this step allowing the switch rails to move freely.
(3) The switch rail is moved back into position at the drives by applying the drive forces of 6 kN. The final state of the switch rail with the foreign object can be seen in Figure 9.
(4) The state of the switch rail obtained during static equilibrium is then used as the initial state for subsequent dynamic simulations. The train negotiates the switch at a speed of 100 km/h in the through (straight) route in the facing move. The resulting wheel–rail contact forces, foreign object deformation and wheel lift are studied for all cases of foreign object variations.

By examining these parameters, the simulation aims to provide insights into the behaviour of the system and evaluate the effects of different foreign object variations on the overall dynamics of the switch rail and the derailment risk of the vehicle.

Simulation outcomes

Validation

The model's validation involved a comparison of the lateral displacement of the switch rail between the drives to field measurements, and FE model results obtained from [11]. An aluminium spacer of certain length resulting in a gauge narrowing of 30 mm at the top of the switch was used in the tests which is assumed to represent a worst-case scenario. Figure 10 clearly indicates that the results obtained from the Simpack model align

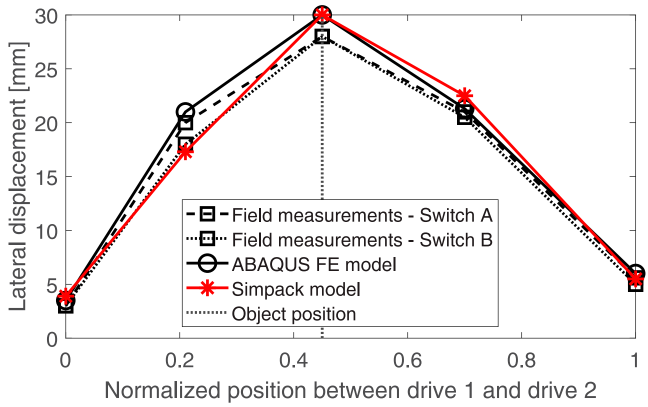

Figure 10. Lateral displacements of switch rail along longitudinal direction obtained by Simpack simulations, field tests and ABAQUS FE simulations. The longitudinal position between drives 1 and 2 is normalized by the distance between the drives. Results for field measurements and ABAQUS FE simulations are taken from [11].

well with both field test measurements and FE simulation results. The switch rail deformations observed in the Simpack simulations fall within acceptable tolerance limits, further confirming the accuracy and reliability of the model.

Lateral forces and displacements at foreign object

Lateral forces and displacements at the location of the foreign object when a train runs through the switch are illustrated in Figure 11. In the linear object case, the lateral force peak at approximately 140 kN, exerting a significant amount of force. Lateral displacement variations in the linear case are small at the object due to the linear stiffness. The ballast stone exhibits a distinctive behaviour compared to the linear case. Once the force reaches 40 kN, there is a sudden drop, resulting in complete loss of stiffness at the object. This leads to large lateral displacements at the foreign object resulting in the switch rail going back into contact with the stock rail and thus eliminating the gauge narrowing.

Wheel–rail contact forces

The train follows the through route, causing the right wheel to ride on the switch rail while the left wheel rides on the stock rail. In Figure 12, it is evident that in the linear case, the wheelset experiences higher dynamic variations of wheel–rail contact forces compared to the ballast stone case. On reaching the foreign object position, i.e. 3.9 m, due to the gauge narrowing induced by the object, the wheelset experiences high lateral and vertical forces until it crosses the switch. High lateral forces can lead to increased risk of derailment by flange climbing and induce damage to the rail itself. On the other hand, the ballast stone case exhibits minimal variation in contact forces due to the early failure of the ballast stone.

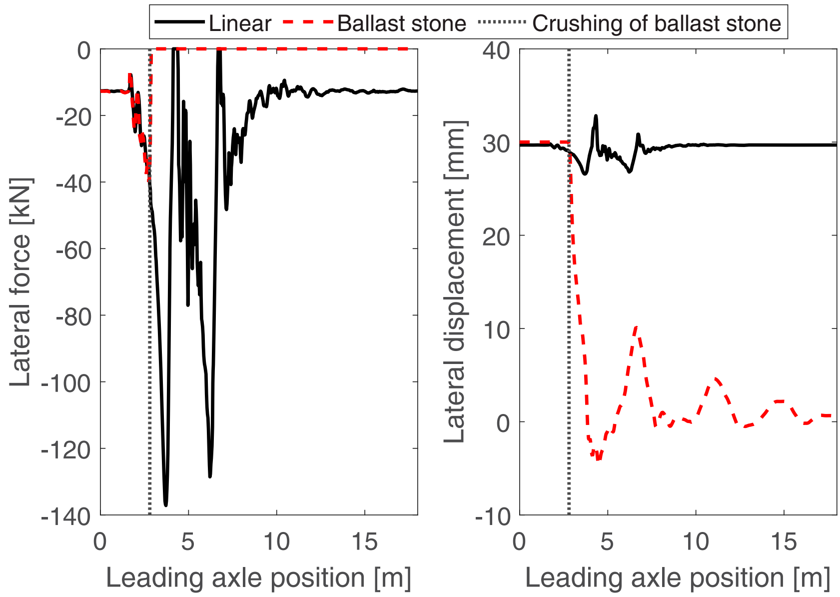

Figure 11. Lateral forces and displacements experienced by two types of foreign objects during a simulated vehicle passage.

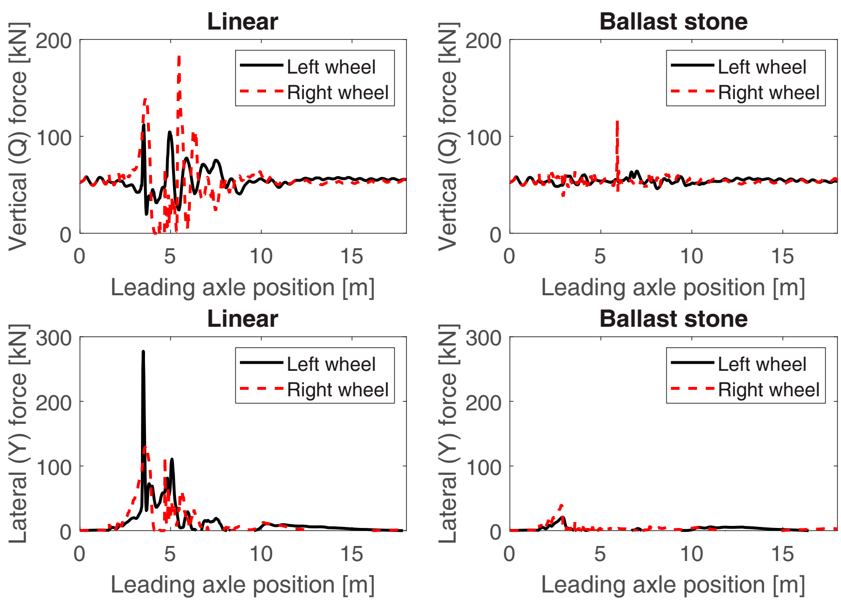

Figure 12. Variation in vertical (Q) and lateral (Y) forces experienced by the leading left and right wheels for two types of foreign objects during a simulated vehicle passage. A positive lateral wheel force is pushing the rail outwards away from the track centre.

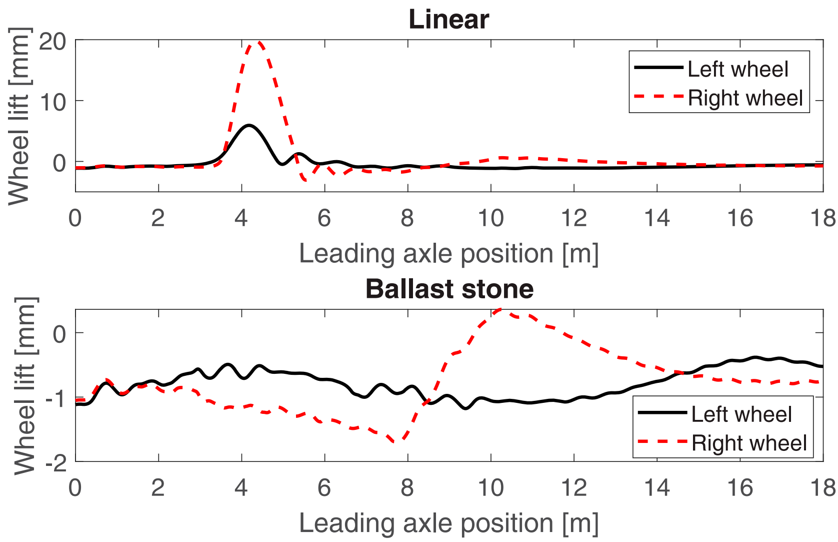

Figure 13. Wheel lift relative to ground for left and right leading wheels for linear object and ballast stone scenarios during a vehicle passage. Note the different scales.

Derailment risk evaluation by wheel lift criterion

The wheel lift criterion is utilised to assess the derailment risk. In [43], 6 mm of wheel lift was taken as a limit corresponding to a significant derailment risk. This criterion was utilised in this study. The wheel lift is defined as the relative vertical displacement between the top of rail and the nominal running circle of the wheel. Examining Figure 13, it becomes evident that only in the linear case does the left wheel lift significantly go above this limit. Consequently, the linear case poses an increased likelihood of derailment. Conversely, the presence of a ballast stone leads to minimum wheel lift. Although the risk of derailment in this case is low, the wheels are in hard flange contact on both sides as the nominal lateral clearance of the wheelset is around 15–20 mm (and maximum gauge narrowing is 30 mm before crushing of the ballast stone).

Switch rail rotation

Lateral displacement of switch rail top and bottom (at object location) for linear and ballast object formulations are presented in Figure 14. From the plots, it can be noted that in the ballast object formulation, both top and bottom of the rail move together, since the ballast stone is crushed and thereafter the switch rail can move freely. In the linear case on the other hand, the top of switch rail moves considerably more when compared to the bottom of the rail during wheel passage, inducing torsion in the switch rail. Even with a switch rail rotation (α) of around 3.5°, gauge narrowing at the top is still above the safety limit of 15 mm [10]. Switch rail rotation due to rail flexibility reduces the effective gauge narrowing and thereby reduces the risk of derailment.

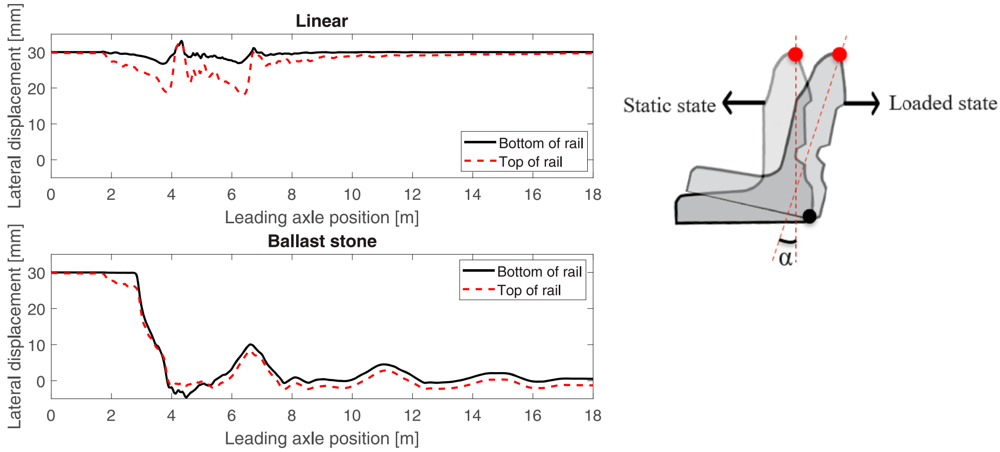

Figure 14. Left: Lateral displacements of bottom and top of rail for linear object and ballast stone cases. Right: Illustration of rail rotation (α) caused by gauge narrowing introduced by foreign object (static state) and during passage of train (loaded state).

Link contribution

Force experienced by the links during train passage for both object formulations are shown in Figure 15. Link-2 is the closest to the foreign object position and experiences a compressive force of 4 kN in the static condition. This means that the object experiences an additional compressive force of 4 kN because of the links. This contributes to the crushing of the ballast stone. Without the links, it would be slightly more difficult for the passing train to crush the stone which has also been verified in simulations. For the linear object case, it can be observed that the forces return to the initial values after the vehicle has passed while in the ballast stone case the object is crushed, and the link forces are around zero.

Parameters that influence derailment risk

Several factors can influence the derailment risk in railway switches in addition to foreign objects. It is therefore of interest to study the influence of such parameters to see how they can together with foreign objects influence the derailment risk. The classic derailment criterion by Nadal [44,45] defines derailment risk in terms of the Y/Q-force ratio (lateral over vertical wheel force) with a limit defined as a function of contact angle and friction coefficient. From this criterion, it can be directly inferred that the wheel–rail contact friction influences derailment risk. Factors that reduce the Q-force or increase the Y-force would also increase derailment risk. It can therefore be expected that a reduced axle load increases derailment risk in gauge narrowing situations where high lateral loads can be generated for kinematic reasons. Further it can be expected that higher speeds and increased fluctuations in dynamic wheel–rail contact loads can increase derailment risk. It is also well known that track irregularities can influence derailment risk and hence there are limits on track irregularities as defined in EN13848-5 [46]. In the European project D-Rail [43], it was found that in particular lateral and twist irregularities could increase derailment risk

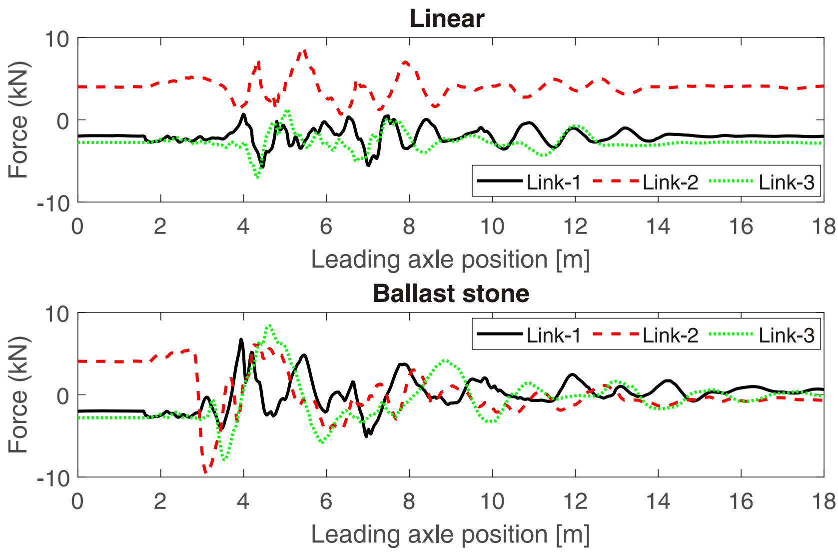

Figure 15. Forces experienced by the links in linear and ballast cases. Black solid lines indicate results from link-1, while red and green curves indicate links 2 and 3 respectively (counting from the left in Figures 1 and 5). Forces are positive in compression.

in switches as they can combine to decrease vertical and increase lateral wheel–rail contact forces. In the D-Rail project it was also investigated how vehicle parameters and vehicle load imbalances could influence derailment risk, but that is out of the scope for the present investigations. The traffic situation itself can influence the derailment risk, as an S&C can see traffic in both the through and diverging routes and in facing and trailing direction. To quantify the influence of these additional factors, the following sections will study the influence of wheel–rail friction, axle load and speed in a parametric study, the influence of track irregularities and the influence of traffic in the trailing move. The studies are performed for traffic in the through route. Traffic in the diverging route, and hence a curve, could be the more critical in terms of derailment risk in some situations in absolute terms, but the qualitative influence from parameters is expected to be similar and the through route is the most interesting from a traffic volume perspective.

W/r friction coefficient, axle load and vehicle speed

The influence of vehicle speed is investigated for speed levels 20, 100 and 160 km/h. Similarly wheel–rail friction coefficients of 0.1, 0.4 and 0.7, and axle loads of 5 t, 11 t and 25 t are used. The 5 t axle load corresponds to an empty freight wagon, 11 t corresponds to a passenger vehicle and 25 t to a locomotive.[1] For the vehicle speed and w/r friction coefficient investigations, the axle load is assumed to be 11 t. For all the cases, the friction coefficient between the switch rail and slide chair is kept constant at 0.1. Both object formulations are investigated in this parametric study. The default values are axle load 11 t, w/r friction coefficient 0.4 and vehicle speed of 100 km/h. The influence of different parameters on the wheel lift for a ballast stone and linear objects is presented in Tables 2 and 3 respectively.

Table 2. Influence of w/r friction coefficient, vehicle speed and axle load on the wheel lift for a ballast stone case.

Axle load [t]	5	11	25
Wheel lift [mm]	0.76	0.37	0
Vehicle speed [km/h]	20	100	160
Wheel lift [mm]	0.106	0.37	0.25
w/r Friction coefficient	0.1	0.4	0.7
Wheel lift [mm]	0.12	0.37	0.7

Table 3. Influence of w/r friction coefficient, vehicle speed and axle load on the wheel lift for a linear object case.

Axle load [t]	5	11	25
Wheel lift [mm]	21.64	19.69	14.84
Vehicle speed [km/h]	20	100	160
Wheel lift [mm]	13.8	19.6	25.94
w/r Friction coefficient	0.1	0.4	0.7
Wheel lift [mm]	11.19	19.6	17.7

The results from the ballast stone case indicate that none of the considered parameters have a major impact on the derailment risk. This is because in all cases, the ballast stone is crushed even before the front wheelset reaches the object position. In the linear case on the other hand, axle load and vehicle speed have a linear relationship while it is non-linear in the case of w/r friction coefficient. A fivefold increase in axle load results in the wheel lift decreasing by 31% but is still above the safety limit of 6 mm. For the case of w/r friction coefficients of 0.1 and 0.4 (refer to Figure 13), the wheel lift is unilateral and the right wheel experiences maximum wheel lift. Wheel lift is bilateral and is more even between both the wheels in the case of 0.7 w/r friction coefficient, which means that the lift of the axle's centre of mass is highest in this case. In conclusion, the influence of parameters is dependent on the type of foreign object that is stuck between the switch and the stock rail.

Switch rail irregularities

This section evaluates the impact of track irregularities on derailment risk in the presence of a trapped foreign object. The focus is on twist and lateral track irregularities as these are the most influential in terms of derailment risk in switches [43], especially when combined. Worst-case point faults are created by introducing track irregularities with a short 6 m wavelength irregularity with peak amplitude at the object location. The amplitudes correspond to the intervention limits of the EN 13848-5 [46] for straight track and 100 km/h traffic, which is 12 mm of lateral track irregularity and 5 mm/m of track twist. The maximum track twist then becomes 15 mm with a measurement base length of 3 m (the track twist goes from zero to peak and back to zero over 6 m). The sinusoidal basis function used to describe the track irregularities is shown in Figure 16. Here, a 15-mm linear foreign object is considered, as it closely represents a real-case scenario [11]. The derailment risk is assessed using the wheel lift criterion.

In total, three cases of track irregularities are investigated: track twist and lateral irregularities separate and combined. A track twist with peak amplitude of 15 mm over 3 m is

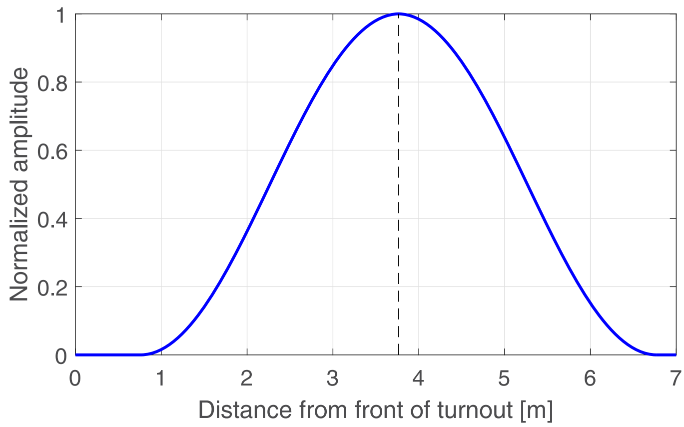

Figure 16. Sinusoidal basis function with 6 m wavelength for track irregularities with peak amplitude at object location. The amplitude is scaled based on the type of irregularity (twist, lateral or combined).

introduced on the right-hand rails (switch rail and stock rail) at the position of the foreign object. This is realised by introducing a combination of positive track roll (Φ) and positive vertical excitation at the track centreline using the basis function in Figure 16. As a result, the left stock rail remains horizontal while the right switch rail moves downward to create the track twist. Observations from wheel lift results from Figure 17 (top), show that the applied track twist does not result in an increase in derailment risk as the wheel lift is minimal on both wheels.

Lateral track irregularities are also introduced using the basis function in Figure 16, with a maximum amplitude of 12 mm at the location of the foreign object. The track is excited in the negative y-direction (moving the rails on the object side inwards and outwards on the opposite side), representing the worst-case scenario where the lateral irregularity further increases the lateral force on the switch rail. Results in Figure 17 (middle) indicate that wheel lift on both wheels are well below the derailment limit of 6 mm. Compared to the nominal case (without irregularity), maximum wheel lift increases marginally on the right wheel due to the irregularity.

Finally, a combination of track twist and lateral irregularities is evaluated. From Figure 17 (bottom), it can be seen that the left wheel experiences maximum wheel lift in this case. The combination of both the lateral and track twist irregularities leads to marginal increase in the wheel lift compared to individual irregularity cases.

Trailing move

This section evaluates the derailment risk when a train approaching the switch in a trailing move interacts with the trapped foreign object. Setup for the trailing move simulations is as shown in Figure 18. Tangent track (21.9 m) has been added before the start of the switch to ensure a smooth transition zone. The passenger vehicle model (11 t) is approaching the switch at 100 km/h and the resulting wheel lift for the linear object and ballast stone formulations (foreign object size 30 mm) are as seen in Figure 19. For the linear object, the wheel lift is above the safety limit in both facing and trailing move. In the ballast stone scenario

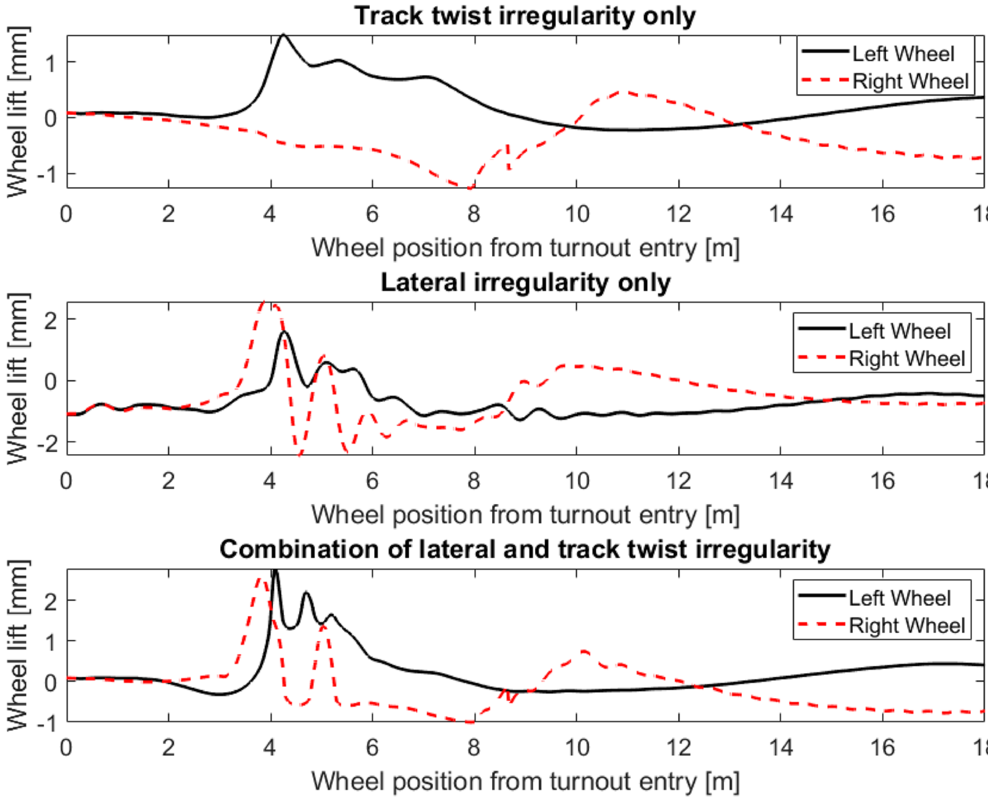

Figure 17. Wheel lift against leading axle position for different types of irregularities. Note the different scales.

on the other hand, the wheel lift is well within the safety limit. Hence, both trailing and facing move show similar trends for both foreign object formulations.

Derailment limit in terms of gauge narrowing

This section explores the derailment limit as a function of gauge narrowing, aiming to support the potential relaxation of current regulations on accepted gauge narrowing limits. According to Swedish standards, the accepted gauge narrowing limit is 15 mm [10] as monitored by the TKK sensors. Findings from previous section have shown that ballast stones measuring 30 mm, when acting as foreign objects, are crushed by the lateral forces exerted by the train. This indicates that ballast stones of that size do not pose a derailment risk under normal conditions. However, when metal or other infinitely strong foreign objects of 30 mm are present, wheel lift exceeds the safety limit. Given this worst-case scenario, it becomes essential to investigate the maximum safe gauge narrowing with such strong objects in place. This investigation could help in reassessing or softening the control limits of the system which will potentially help in improving the efficiency of the railway system with fewer out of control switches.

To this end, dynamic simulations for linear object of sizes from 5 to 35 mm with a step size of 5 mm are carried out. In Figure 20, the maximum wheel lift for the different effective

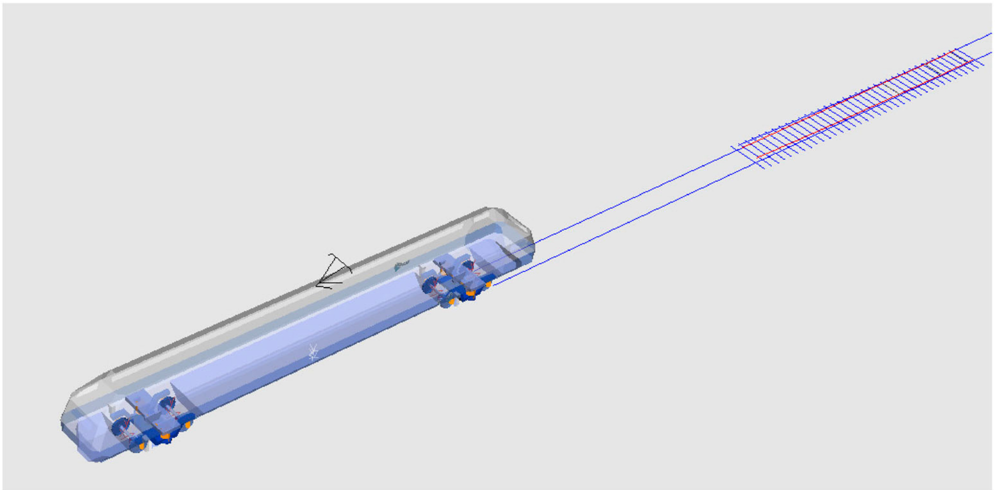

Figure 18. Setup of the MBS model for trailing move in Simpack.

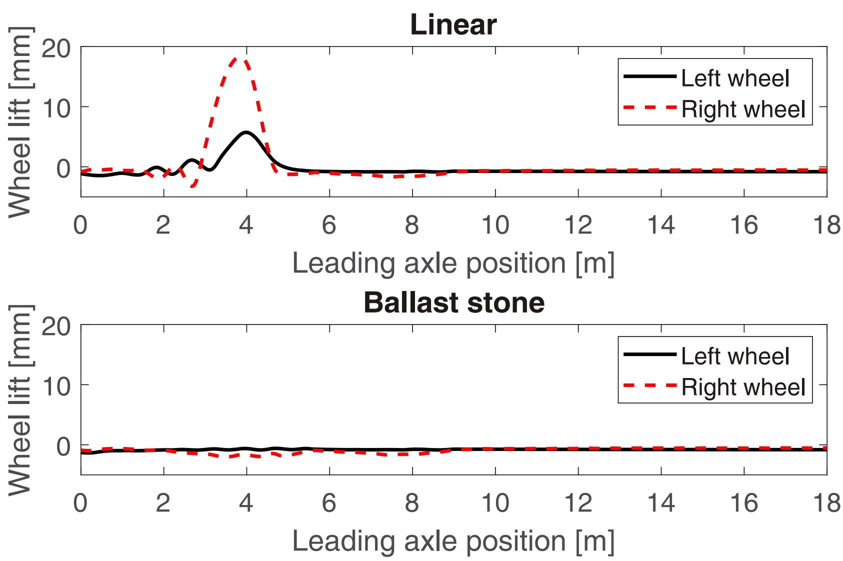

Figure 19. Wheel lift against leading axle position for linear and ballast object formulations in the trailing move.

object sizes is plotted. Maximum wheel lift goes above the safety limit when the object size and the resulting gauge narrowing are in between 15 and 20 mm. Hence the current gauge narrowing limit of 15 mm and the current TKK sensor limits of 13 mm to enforce this are appropriate.

Conclusion

This paper has assessed the derailment risk due to gauge narrowing caused by foreign objects getting stuck between switch and stock rails in railway switches. MBS is employed

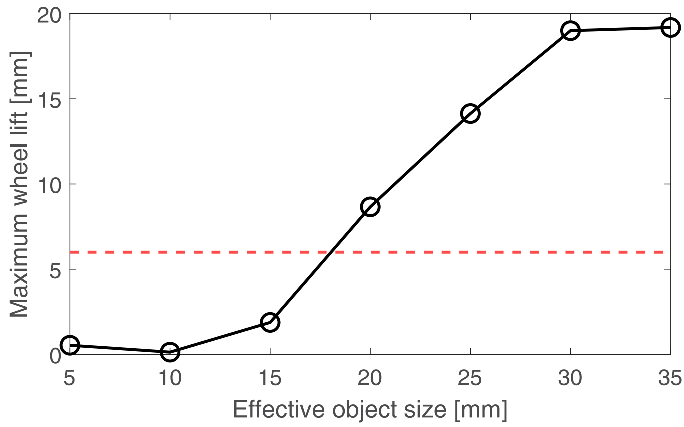

Figure 20. Maximum wheel lift as a function of effective object size. Red line indicates the 6 mm wheel lift safety limit.

to simulate the vehicle–switch interaction in the presence of a foreign object. Investigations have been carried out for linear and ballast stone object formulations and results show that according to a wheel lift-based derailment criterion. This is because there is a derailment risk for linear objects while the risk is very low for ballast stone. Since ballast stones will be crushed due to lateral forces from the train.

The robustness of the results has been investigated through parametric studies (accounting for axle load, wheel–rail friction coefficient and speed). For the ballast stone case, none of the considered parameters were found to have a major impact on the wheel lift. This is because in all cases the ballast stone gets crushed even before the front wheelset reaches the object position. In the linear object case, vehicle speed and w/r friction coefficient increase the risk of derailment while it decreases with axle load.

The derailment limit in terms of gauge narrowing is investigated in a bid to support the potential of TKK margins while maintaining safety. Since the linear object case is the worst-case scenario, investigations are carried out for this object type. Observations from the wheel lift results indicate that it exceeds the safety limit when the gauge narrowing is between 15 and 20 mm for the considered vehicle parameters. Hence, the acceptable gauge narrowing that can be tolerated without derailment (linear object formulation) is between 15 and 20 mm. The safety margin of 15 mm, therefore, seems to be an acceptable safe gauge narrowing limit. This means that the TKK working limit at 13 mm is acceptable. If only ballast stone cases are considered, the TKK can be omitted from the switch system. The MBS model was extended to determine the influence of track irregularities on the derailment risk. Simulations were carried out for twist and lateral track irregularities corresponding to intervention limits for point faults, and the results show that a combination of lateral and track twist irregularities leads to a marginal increase in the wheel lift but still well within the safety limit for an object size of 15 mm. Further studies on the probability of objects with linear properties getting stuck between switch and stock rail are necessary to decide how the TKK affects the overall safety.

Note

1. Locomotive has different running gear when compared to a passenger vehicle model, but in the considered scenario only the axle load of the locomotive is considered.

Disclosure statement

No potential conflict of interest was reported by the author(s).

Funding

The current work is part of the activities within the Centre of Excellence CHARMEC (CHAlmers Railway MEChanics, www.chalmers.se/charmec). The work is mainly funded by Trafikverket (Swedish transport administration) under contract number 2021/53614 and partly by Project 101102001-FP2 - R2DATO in Europe's Rail and Horizon Europe. The computations were enabled by resources provided by the National Academic Infrastructure for Supercomputing in Sweden (NAISS) and the Swedish National Infrastructure for Computing (SNIC) at C3SE partially funded by the Swedish Research Council through grant agreement no. 2022-06725.

ORCID

Sucheth K. K. Bysani http://orcid.org/0000-0003-4026-8821
Björn A. Pålsson http://orcid.org/0000-0002-2237-8560
Elena Kabo http://orcid.org/0000-0002-9779-135X

References

[1] Johansson A, Pålsson B, Ekh M, et al. Simulation of wheel–rail contact and damage in switches & crossings. Wear. 2011;271(1–2):472–481. doi:10.1016/j.wear.2010.10.014
[2] Pålsson B. Optimization of railway switches and crossings [doctoral thesis]. Gothenburg, Sweden: Chalmers University of Technology, Department of Mechanics and Maritime Sciences; 2014. 57 pp.
[3] Kassa E, Nielsen JCO. Dynamic interaction between train and railway turnout: full-scale field test and validation of simulation models. Veh Syst Dyn. 2008;46(sup1):521–534. doi:10.1080/00423110801993144
[4] Trafikverket. Säkerhetsbesiktning av fasta järnvägsanläggningar. TDOK. 2022;2014:0240, 125 pp. [in Swedish].
[5] Andersson D, Carlvik F, Kronvall-Bjelkengren F, et al. Risk analysis for rail transport – a study on the possibility of improvements for TKK and load imbalance based on risk analysis [Bachelor thesis]. Chalmers University of Technology, MMSX2018-27; 2018. 86 pp.
[6] Trafikverket. Spårväxel. Report, TRVINFRA-00017; 2021. 160 pp. [in Swedish].
[7] Blomqvist M, Blomqvist M. Problems related to switches: future proposals for action. BSC thesis. KTH Royal University of Technology; 2013. 68 pp.
[8] Nilsson T, Andersson R. The problems surrounding Easyswitch and the 60E switch standard. MSc. Lund, Sweden: Lund University; 2015. 96 pp.
[9] Paulsson B, Ekberg A. More robust switches through improved control of the switch rail. Chalmers University of Technology, Department of Mechanics and Maritime Sciences; 2022. Research report 2022:01. 48 pp.
[10] ORE C138 RP1. Permissible maximum values for the Y- and Q-forces as well as the ratio Y/Q. Utrecht, Netherlands: International Union of Railways Office of Research and Experiments; 1977. 78 pp.
[11] Bysani SKK, Pålsson BA, Kabo E, et al. The influence of trapped foreign objects on railway switch control investigated by simulations and field tests. Submitted for international publication; 2024. 20 pp.

[12] https://news.cision.com/se/banverket/r/jarnvagen-atergar-successivt-tillnormallage, c137760, 2023-02-10.
[13] Sebes M, Chollet H, Monteiro E, et al. Adaptation of the semi-Hertzian method to wheel/rail contact in turnouts. In: Dynamics of vehicles on roads and tracks: Proceedings of the 24th Symposium of the International Association for Vehicle System Dynamics (IAVSD2015), 1st ed., Graz, Austria; 17–21 August 2015. CRC Press; 2016. p. 1367–1376.
[14] Antunes P, Magalhaes H, Ambrosio J, et al. A co-simulation approach to the wheel-rail contact with flexible railway track. Multibody Syst Dyn. 2019;45(2):245–272. doi:10.1007/s11044-018-09646-0
[15] Shih JY, Ambur R, Dixon R. Developing a detailed multi-body dynamic model of a turnout based on its finite element model. Veh Syst Dyn. 2020;2020:15.
[16] Jorge P, Bezin Y, Grossoni I, et al. Modelling track flexibility in turnouts using MBS approach. In: Klomp M, Bruzelius F, Nielsen J, et al., editors. Advances in dynamics of vehicles on roads and tracks. IAVSD 2019. Cham: Springer; 2020. 8 pp.
[17] Kassa E, Nielsen JCO. Dynamic train-turnout interaction in an extended frequency range using a detailed model of track dynamics. J Sound Vib. 2009;320(4–5):893–914. doi:10.1016/j.jsv.2008.08.028
[18] Chen JY, Chen R, Xu JM, et al. Simulation of vehicle-turnout coupled dynamics considering the flexibility of wheelsets and turnouts. Veh Syst Dyn. 2023;61(3):739–764. doi:10.1080/00423114.2021.2014898
[19] Bruni S, Anastasopoulos I, Alfi S, et al. Train-induced vibrations on urban metro and tram turnouts. J Transp Eng ASCE. 2009;135(7):397–405. doi:10.1061/(ASCE)TE.1943-5436.0000008
[20] Alfi S, Bruni S. Mathematical modelling of train-turnout interaction. Veh Syst Dyn. 2009;47(5):551–574. doi:10.1080/00423110802245015
[21] Vilhelmson H, Pålsson BA, Nielsen JCO, et al. Dynamic vehicle–track interaction and structural loading in a crossing panel–calibration and assessment of a model with a 3D representation of the crossing rail. Veh Syst Dyn. 2024;62(12):3168–3190.
[22] Milošević MDG, Pålsson BA, Nissen A, et al. Reconstruction of sleeper displacements from measured accelerations for model-based condition monitoring of railway crossing panels. Mech Syst Signal Process. 2023;192:1–21.
[23] Bezin Y, Iwnicki SD, Cavalletti M, et al. An investigation of sleeper voids using a flexible track model integrated with railway multi-body dynamics. Proc Inst Mech Eng Pt F J Rail Rapid Transit. 2009;223(6):597–607. doi:10.1243/09544097JRRT276
[24] Sebès M, Bezin Y. Considering the interaction of switch and stock rails in modelling vehicle–track interaction in a switch panel diverging route. Veh Syst Dyn. 2021;61(3):765–781. doi:10.1080/00423114.2021.1947510
[25] Pillai N, Shih JY, Roberts C. Evaluation of numerical simulation approaches for simulating train–track interactions and predicting rail damage in railway switches and crossings (S&Cs). Infrastructures (Basel). 2021;6(2):28. doi:10.3390/infrastructures6020028
[26] Pålsson BA, Ambur R, Sebès M, et al. A comparison of track model formulations for simulation of dynamic vehicle–track interaction in switches and crossings. Veh Syst Dyn. 2023;61(3):698–724. doi:10.1080/00423114.2021.1983183
[27] Dutta S, Harrison T, Ward CP, et al. A new approach to railway track switch actuation: dynamic simulation and control of a self-adjusting switch. Proc Inst Mech Eng Pt F J Rail Rapid Transit. 2020;234(7):779–790. doi:10.1177/0954409719868129
[28] Dutta S, Harrison T, Sarmiento-Carnevali M, et al. Modelling and controller design for self-adjusting railway track switch system. Proceedings of 7th Transport Research Arena TRA2018, Vienna, Austria; 2018. 15 pp.
[29] Simpack. Version 2022x.4. Dassault Systemes; 2022. Available from: https://www.3ds.com/
[30] ABAQUS. Abaqus analysis user's manual, Simulia, Dassault Systems; 2019.
[31] Li L, Dutta S, Dixon R, et al. Railway track switch simulation: a new dynamic model for studying actuator and switch blade dynamics. Proc Inst Mech Eng Pt F J Rail Rapid Transit. 2023;237(6):775–783. doi:10.1177/09544097221141741

[32] Dutta S, Harrison T, Ward C, et al. A framework for dynamic modelling of railway track switches considering the switch blades, actuators and control systems. Railway Eng Sci. 2024;32(2):162–176. doi:10.1007/s40534-023-00324-2
[33] Wang P, Lai J, Liao T, et al. Assessment of derailment risk in railway turnouts through quasi-static analysis and dynamic simulation. Proc Inst Mech Eng Pt F J Rail Rapid Transit. 2022;236(4):434–446. doi:10.1177/09544097211024016
[34] Lai J, Xu J, Chen Y, et al. Evaluation of dynamic derailment in a railway switch considering the longitudinal impacts caused by vehicle retarder. Proc Inst Mech Eng Pt F J Rail Rapid Transit. 2023;237(6):806–817. doi:10.1177/09544097221138391
[35] Jiang Y, Chi M, Yang J, et al. Investigation on the mechanism and measures of derailment of empty freight train passing a turnout in the diverging route. Eng Fail Anal. 2024;156:28.
[36] Lai J, Xu J, Liao T, et al. Investigation on train dynamic derailment in railway turnouts caused by track failure. Eng Fail Anal. 2022;134:22.
[37] Iwnicki S. Manchester benchmarks for rail vehicle simulation. Veh Syst Dyn. 1998;30(3–4): 295–313. doi:10.1080/00423119808969454
[38] Craig RR, Bampton MCC. Coupling of substructures for dynamic analyses. AIAA J. 1968;6(7):1313–1319. doi:10.2514/3.4741
[39] Ulan-Kvitberg C, Daley CG, Kim H-W, et al. Crushing characteristics of dry, wetted and submerged ice, ISOPE International Ocean and Polar Engineering Conference. ISOPE; 2011. 27 pp.
[40] Petrovic JJ. Review mechanical properties of ice and snow. J Mater Sci. 2003;38(1):1–6. doi:10.1023/A:1021145312108
[41] Wang B, Martin U, Rapp S. Discrete element modeling of the single-particle crushing test for ballast stones. Comput Geotech. 2017;88:61–73. doi:10.1016/j.compgeo.2017.03.007
[42] Hafström R. Loading and crushing of trapped ballast stones [MSc thesis]. Gothenburg, Sweden: Chalmers University of Technology; 2020. 45 pp.
[43] Braghin F, Ekberg A, Pålsson BA, et al. D-Rail deliverable 3.2 – analysis and mitigation of derailment, assessment and commercial impact. 120 pp.
[44] Andersson E, Berg M, Stichel S, et al. Rail vehicle dynamics. Stockholm: Railway Group KTH, Kungliga Tekniska högskolan; 2014. 225 pp.
[45] Iwnicki S. Handbook of railway vehicle dynamics. Boca Raton (FL): CRC Taylor & Francis; 2006. 475 pp.
[46] Svenska institutet för standarder. EN 13848-5, railway applications – track – track geometry quality – part 5: geometric quality levels – plain line, switches and crossings; 2017.